

# Study of Bremsstrahlung Finding at the Belle II Experiment

Patrick Ecker

Bachelorthesis

26.01.2018

Institut für Experimentelle Teilchenphysik (ETP)

Advisor: Prof. Dr. Florian Bernlochner  
Coadvisor: Dr. Thomas Hauth

Editing time: 01.05.2017 – 26.01.2018



# Studien zur Bremsstrahlungsfindung am Belle II Experiment

Patrick Ecker

Bachelorarbeit

26.01.2018

Institut für Experimentelle Teilchenphysik (ETP)

Referent: Prof. Dr. Florian Bernlochner  
Korreferent: Dr. Thomas Hauth

Editing time: 01.05.2017 – 26.01.2018



---

Ich versichere wahrheitsgemäß, die Arbeit selbstständig angefertigt, alle benutzten Hilfsmittel vollständig und genau angegeben und alles kenntlich gemacht zu haben, was aus Arbeiten anderer unverändert oder mit Abänderungen entnommen wurde.

**Karlsruhe, 26.01.2018**

.....  
**(Patrick Ecker)**



# Contents

<b>1</b>	<b>Introduction</b>	<b>1</b>
<b>2</b>	<b>The Belle II Experiment</b>	<b>3</b>
2.1	SuperKEKB . . . . .	3
2.2	Detector . . . . .	3
2.3	The Software Framework . . . . .	7
<b>3</b>	<b>Bremsstrahlung Effects</b>	<b>9</b>
3.1	Bremsstrahlung . . . . .	9
3.2	Characteristics at Belle II . . . . .	9
<b>4</b>	<b>New Approach on Bremsstrahlung Finding</b>	<b>13</b>
4.1	The Belle Recovery Method . . . . .	13
4.2	Idea . . . . .	13
4.3	ECL Position Resolution . . . . .	14
4.4	Implementation . . . . .	17
<b>5</b>	<b>Evaluation</b>	<b>21</b>
5.1	Module Efficiency . . . . .	21
5.2	Photon Vertex Reconstruction . . . . .	24
5.3	Comparison to the Belle Method . . . . .	27
<b>6</b>	<b>Summary</b>	<b>29</b>



# 1. Introduction

One of the great mysteries in todays physics is the dominance of matter over anti-matter in the universe. The standard model of particle physics delivers no explanation for the related baryon asymmetry after the big bang. The Belle II experiment is constructed to get answers for still unexplained fundamental puzzles like this asymmetry.

The Belle II experiment is an update of the Belle experiment, which was operated at the KEKB collider in Tsukuba, Japan, till 2010. The main purpose of Belle was the verification of the theory of CP-violation described by the nobel-prize winners Makoto Kobayashi and Toshihide Maskawa. Their theory delivers an explanation for the previously observed CP-violation in Kaon-decays and predicted a third flavor generation. Belle was able to observe the CP-violation in the way it is described in the Kobayashi-Maskawa-theory [1]. After the confirmation of the KM-theory the KEKB collider was updated to SuperKEKB. SuperKEKB is an asymmetric electron-positron collider with a center-of-mass energy adjusted on the  $\Upsilon(4S)$  resonance. The updated collider delivers a much higher luminosity than its predecessor, which requires a redesign and improvement of the Belle detector.

Therefore the Belle II detector is designed and build since 2010. Due to the great amount of data, which can be taken with the newly designed detector, it is possible to make exact measurements in the field of heavy flavor physics [2], like for example the observation of rare decays. The detector also has the purpose to verify theories beyond the standard model of particle physics. This theories are able to answer the open questions of the standard model, just like the matter-antimatter asymmetry, which can in the measured size not be explained by the CP-violation, observed at Belle. An overview of the experimental setup is given in Chapter 2.

In the course of the detector update, the software of the Belle experiment has been totally rewritten. To make more exact measurements an improved energy determination of the electrons in the detector is desired. Therefore, this thesis deals with the recovery of the energy, leptons have lost via bremsstrahlung as they pass the layers of the vertex detector. The recovery of this energy should lead to improvements in the track fitting and therefore in the vertex reconstruction.

To develop a method for the bremsstrahlung recovery, more detailed information about the bremsstrahlung characteristics at Belle II is needed. Therefore Chapter 3 gives an introduction in bremsstrahlung effects and works out the qualities of bremsstrahlung photons in the experiment.

The fact, that the bremsstrahlung photons are mostly emitted at positions where dense material is located, mostly at the inner detector layers, leads to the new approach for the

bremsstrahlung recovery described in Chapter 4.2. Thereby a tangent to the track at each measured hit gets extrapolated to the electromagnetic calorimeter and then the extrapolation gets compared with the position of ECL clusters. This method allows to not only to reconstruct the energy to the bremsstrahlung photon, but also to reconstruct the location where the photon was radiated.

Chapter 5 shows the advantages of the new approach over the one mostly used during off-line reconstruction at the Belle experiment. It also points out the behavior of the method towards different characteristics of the electrons and bremsstrahlung photons.

Finally Chapter 6 summarizes the results of the evaluation and gives an outlook on what still has to be improved at the method, like the implementation of the module in the track fitting algorithm.

## 2. The Belle II Experiment

In this chapter a look on the experimental setup of the Belle II experiment and the SuperKEKB collider is given. The aim is to give an overview of the setup. More detailed information can be gained from the Belle II Technical Design Report [2].

### 2.1 SuperKEKB

SuperKEKB is a particle accelerator operated by the Japanese High-Energy Accelerator Research Organization in Tsukuba, Japan. It is still under construction and constitutes an upgrade to the KEKB accelerator, which was operated from 1998 to 2010. The goal of this update is to get detailed information about unsolved physical problems, like the baryon asymmetry in the early universe. The updated accelerator provides the possibilities to investigate rare decays and therefore explore new physics beyond the standard model. Therefore the plan is to achieve a 40 times higher luminosity with electron-positron collisions than the current world record of  $2.11 \text{ cm}^{-2} \text{ s}^{-1}$ , set by KEKB [3].

SuperKEKB is a so called B-Factory, because the beam energies are chosen in a way so the center-of-mass energy is lying on the  $\Upsilon(4S)$  resonance, which decays in two B-mesons in most cases.

The layout of the accelerator is shown in Figure 2.1. The electrons are accelerated to an energy of 7 GeV in a linear accelerator and are then injected into the High Energy Ring (HER). On the contrary the positrons are accelerated to an energy of 4 GeV and injected in the Low Energy Ring (LER). The different beam energies lead to the fact that SuperKEKB is a asymmetric electron-positron collider.

Due to the higher rate of electron-positron collisions, that comes with the aim of a higher luminosity, the KEKB detector Belle has also to be updated. As a result the Belle II detector is build.

### 2.2 Detector

In order to be able to handle the higher data rates, which comes in connection with the desired luminosity the Belle detector is updated to Belle II. The detector consists of several sub-detectors which are arranged onion-like around the beam pipe. Figure 2.2 shows the schematic structure of the detector. In the following part a short overview about the components is given. The given information and figures are taken from [2], if not otherwise specified.

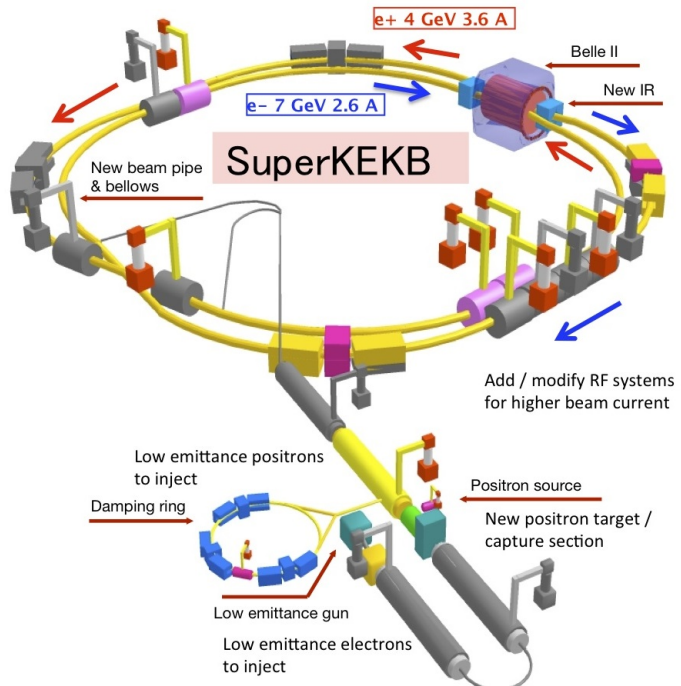


Figure 2.1: Schematic layout of the SuperKEKB accelerator. Taken from [4]

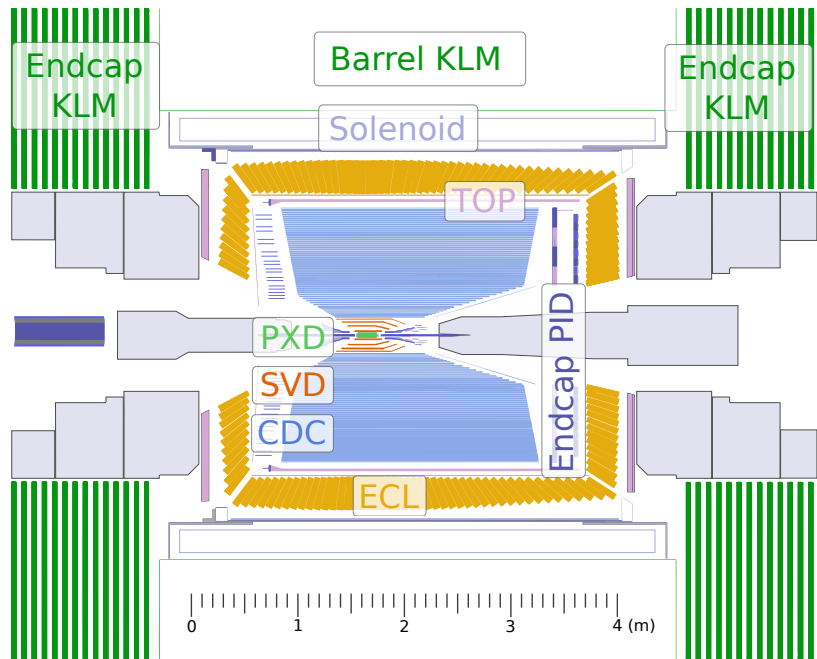


Figure 2.2: Schematic view on the Belle II detector. Taken from [5].

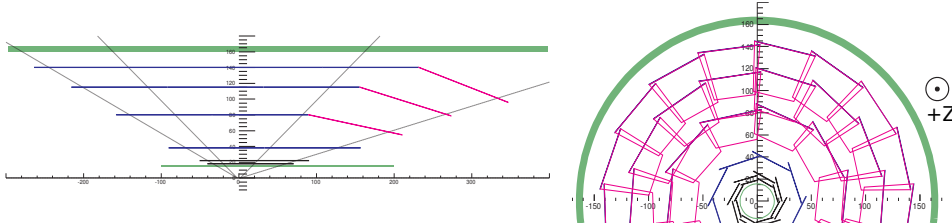


Figure 2.3: Layer configuration of the VXD at the Belle II detector. The thin green line represents the edge of the beam pipe. The PXD layers are presented as black lines, whereas the SVD layers are shown in blue and pink. The inner edge of the CDC can be seen as the thick green line in the figure.

### Beam Pipe

At the interaction region the beam pipe consists of a double layer beryllium cylinder. Beryllium is used to reduce unwanted effects like multiple scattering. A thin gold foil is placed at the inner side of the beam pipe, so synchrotron radiation effects are reduced in the detector.

### Tracking Detectors

With the aim of getting a measurement of time dependent CP-violation in mind, a really good vertex reconstruction is needed. Therefore, a good spatial resolution is required, especially in the innermost parts of the detector. So the Belle II detector has three tracking detectors. A Pixel Detector (PXD) and a Silicon Vertex Detector (SVD) form the vertex detector (VXD). Around these the Central Drift Chamber (CDC) is located. The CDC hits are used to reconstruct the curvature of the track and draw conclusions about the momenta of the particles. Due to the design of the tracking detectors, the Belle II detector has an acceptance region of  $17^\circ < \Theta < 150^\circ$ .

### Pixel Detector

Due to the high luminosity produced at SuperKEKB the innermost detector layers have to handle high hit rates caused by beam-related background and low momentum QED processes. Another challenge is the small radius of the beam pipe at the interaction region (about 10 mm), because the background increases with the inverse square of the radius. These requirements lead to the conclusion that strip detectors are not an option for the innermost tracking detectors. Therefore, for the two layers lying closest to the beam pipe, pixel detectors are used.

To lower effects like multiple-scattering in the detector the pixel detectors should be as thin as possible. For this reason the pixel detectors used at Belle II are based on the DEPFET (DEPlotted Field Effect Transistor) technology [6]. At the chosen layout the readout electronics are located outside the acceptance region of the detector, so their cooling modules are of no consequence for the material budget. Another benefit is the very little power consumption of the sensors so that air cooling becomes sufficient.

### Silicon Vertex Detector

The SVD contains four layers on radii from 38 mm up to 140 mm (Compare Table 2.1). Here silicon stripe detectors are used because the position is far enough away from the beam pipe. The geometry of the SVD and PXD can be seen in Figure 2.3.

Table 2.1: Position of the VXD layers. Taken from the current geometry implementation in the basf2 code.

Layer	Sub-Detector	Radius / mm
1	PXD	14.21
2	PXD	21.79
3	SVD	38.99
4	SVD	80.00
5	SVD	104.00
6	SVD	135.15

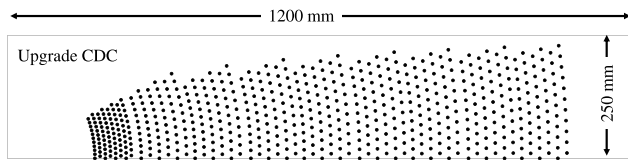


Figure 2.4: Configuration of the sense wires inside the CDC.

### Central Drift Chamber

The CDC has three major purposes. First, it plays an important role in the track reconstruction of charged particles and thus the momentum measurement. The energy loss in its gas volume makes information for particle identification available. In special low momentum tracks which do not reach the particle identification modules at the outer part of the detector can be identified using the information from the CDC. Providing trigger signals for charged particles is also a function of the CDC.

The CDC consists of 14,336 sense wires which are located at radii from 160 mm to 1130 mm. The wire configuration is shown in Figure 2.4. The sense wires are grouped in 56 layers where the distance between the layers is the shortest near to the VXD. A mixture of He and C<sub>2</sub>H<sub>6</sub> is used as filling for the CDC.

### Particle Identification

The particle identification devices are located around the tracking sub-detectors. They are used to separate pions from kaons. For this purpose a Time of Propagation (TOP) Counter and a Aerogel Ring-Imaging Cherenkov detector (ARICH) is used. Both sub-detectors use the Cherenkov effect to distinguish the particle types.

### Electromagnetic Calorimeter

The operating principle of an Electromagnetic Calorimeter is based on bremsstrahlung and electron-positron-pair production. If a particle is hitting the ECL, these two processes are taking place in the calorimeter material and produce an electromagnetic shower. By determining the length of this shower it is possible to get information about the energy the particle had, when hitting the ECL.[7]

There are two kinds of electromagnetic calorimeters to be distinguished: First a calorime-

ter, which consists of alternating layers of absorber and detection material, and second, homogeneous calorimeters, which only consist of mono crystals. These mono crystals serve as absorber and detection material. The Electromagnetic Calorimeter used at the Belle II experiment is a homogeneous calorimeter.

One of the main tasks of the Electromagnetic Calorimeter (ECL) is the detection of neutral particles like  $\pi^0$  or photons in an energy range of 20 MeV up to 4 GeV. Because of that a high energy resolution is needed. The Belle II ECL consists of a 3 m long barrel section with an inner radius of 1.25 m and end caps at  $z = 1.96$  m and  $z = -1.02$  m. The detector contains 6624 CsI(Tl) crystals which have an average size of  $6 \times 6 \text{ cm}^2$  and a length of 30 cm ( $16.1X_0$ ).

### Solenoid Magnet

At Belle II, a superconducting solenoid which generates a homogeneous magnetic field of 1.5 T is used. The homogeneous part of the magnetic field has a cylindrical volume of 3.4 m in diameter and 4.4 m in length.

### $K_L^0$ and $\mu$ Detector

The outermost layer of the detector is represented by the  $K_L$  and muon detector (KLM). It consists of an alternating sandwich of iron plates and active material. In the KLM  $K_L$  mesons can shower hadronically due the supply of 3.9 interaction lengths. The KLM also functions as a magnetic flux return for the solenoid magnet.

## 2.3 The Software Framework

In connection with the detector update there are several new requirements for the software used at the experiment. Therefore, the software for the Belle II experiment was completely rewritten. The new developed software is named BASF2 (Belle 2 Analysis Framework), which is described in [8]. It is based on C++ and Python and uses some external libraries like the ROOT data analysis framework [9].

To handle the large data sets produced by the experiment, a flexible and user-adjustable software is desired. In order to meet this objective the methods, the user wants to apply on the data, are arranged in modules. So the user can chose which modules are utilized by adding them to a path, which represents a chain of modules which are executed step by step. It is also possible to create different paths, which are linked by the return values of their included modules.

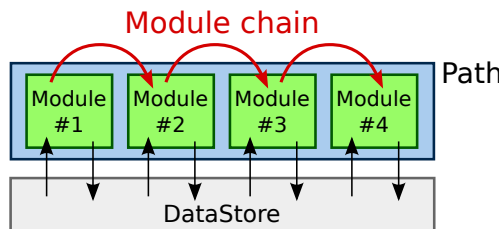


Figure 2.5: Schematic view of the module chain. The 4 modules processed in the path are exchanging data over the DataStore. Figure taken from [8].

The paths are defined in a Python script, a so-called steering file. In this steering file the user can configure the modules and the framework itself. Most of the modules are written in C++ and the algorithms implemented in the modules can be used by other modules as well. Each module has access to the so-called Data Store. From this Data Store the module can read the needed data and after processing save the results. So the Data Store is an instrument for the modules to communicate with each other. This means that a module has access to the results of the modules processed before. The module chain and the interaction of the modules with the Data Store are outlined in Figure 2.5.

## 3. Bremsstrahlung Effects

Before developing a method for the bremsstrahlung recovery, it is important to understand the main characteristics of bremsstrahlung effects and how they occur in the Belle II experiment. Therefore in this chapter a closer look on the bremsstrahlung characteristics is taken.

### 3.1 Bremsstrahlung

Bremsstrahlung is electro-magnetic radiation that occurs if the momentum of a charged particle changes. Bremsstrahlung often takes place in particle accelerators like synchrotron where particles are deflected by a magnetic field. This special effect is called synchrotron radiation. The most relevant effect for this thesis is the energy loss via bremsstrahlung when interacting with matter. In this case the particle is decelerated by the coulomb field of the atoms of the material the particle passes [10].

The probability for a particle emitting bremsstrahlung in materials is proportional to

$$P \sim \frac{q^2 Z^2 E}{m^2}$$

[11] where  $q$  is the charge of the particle, its energy  $E$  and mass  $m$  and the atomic number of the matter  $Z$ . Due to the fact that the probability is proportional to  $\frac{1}{m^2}$ , lighter particles like electrons and positrons have a much higher chance of emitting bremsstrahlung than for example protons or muons.

The energy loss of electrons and positrons, when interacting with matter, is shown in Figure 3.1. As it can be seen there, the energy loss is dominated by bremsstrahlung for energies beyond 400 MeV. Because of the fact that a large number of the electrons in the Belle II experiment have energies lying in this range, a better understanding of the bremsstrahlung effects in the experiment is needed.

The value of the energy the electron has lost by bremsstrahlung is given by the energy of the photon, which is radiated tangentially to the electrons trajectory. This photon then passes through the detector in a straight line and can then, if its energy is high enough, be detected in the ECL.

### 3.2 Characteristics at Belle II

In the Belle II detector the bremsstrahlung effects have an influence on the electron and positron trajectories. Therefore more detailed information of the location of bremsstrahlung

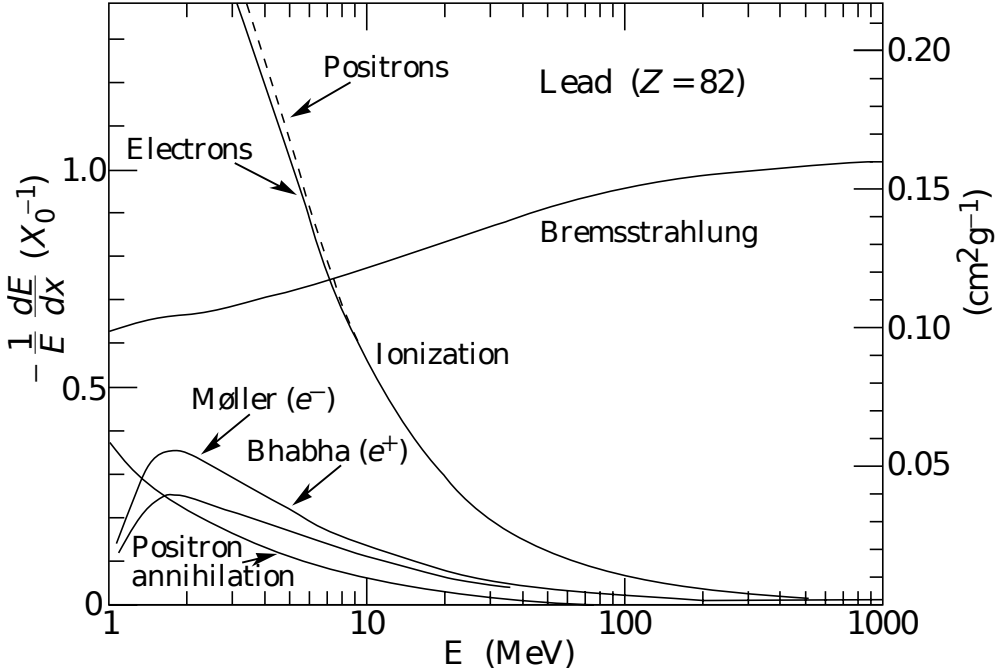


Figure 3.1: Fractional energy loss per radiation length as a function of the electron energy.  
Taken from [12].

emission in the detector and the energy distribution of bremsstrahlung photons is needed. Because of the low probability of other particles than electrons of emitting bremsstrahlung only electrons and positrons are considered for further study in this thesis.

The energy loss via bremsstrahlung results in a kink in the electron trajectory, because of the lost momentum. This effect can be seen as a tail in the momentum resolution of the electrons (Figure 3.2).

In Figure 3.3 the distribution of the bremsstrahlung photon origin is shown. It can clearly be seen that bremsstrahlung photons are emitted at distinct areas in the detector. By taking a closer look on the distribution the layer structure of the VXD is clearly visible. There is also a peak at the edge of the beam pipe where the electron passes material, where the interaction with this leads to bremsstrahlung radiation. The peak at 16 cm can be explained by the edge of the Central Drift Chamber. At this position, the electron also has to pass through a thick layer. The largest amount of all bremsstrahlung photons are emitted within the first 20 cm of the detector. This is also the area where the largest part of material is located. In the CDC we only have an negligible amount of photons, so the main focus when trying to find bremsstrahlung photons should lie on the VXD.

The energy distribution of the bremsstrahlung photons can be seen in Figure 3.4. From special interest is the percentage of bremsstrahlung photons, which have an energy over 10 MeV, because that is the energy threshold for the reconstruction of a ECL cluster. Photons with an energy below this threshold are not from interest in this thesis, because they can not be detected in the ECL and the relative energy loss is small enough to ignore them. About 65% of the photons meet the energy requirement and about 75% of them

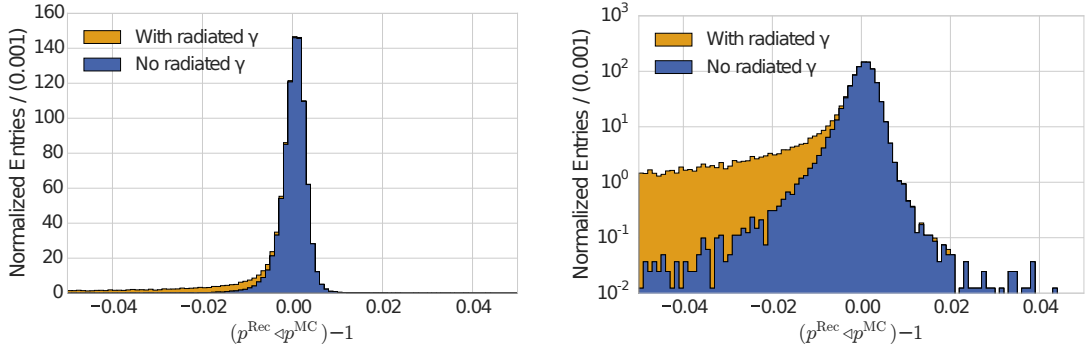


Figure 3.2: Momentum resolution of electrons based on Monte Carlo information. Electrons with no radiated photon with an energy beyond the threshold of 10 MeV are shown in blue. Electrons with at least one radiated photon in orange. For better visualization, the plot on the right hand side has an logarithmic y-axis. Plots are taken from [13].

generate a cluster in the ECL.

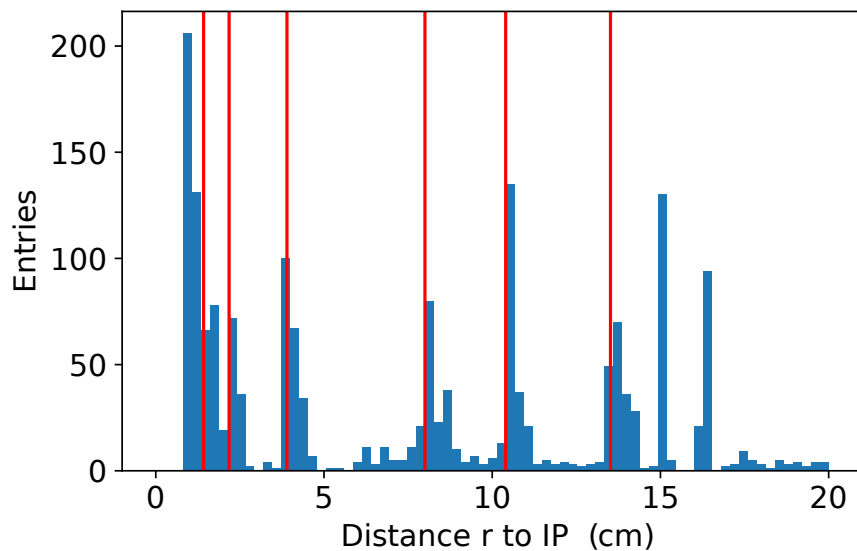


Figure 3.3: Distribution of the bremsstrahlung photon vertex position (blue) from Monte Carlo information in Y(4S)-Events. Radii of the VXD layers (red).

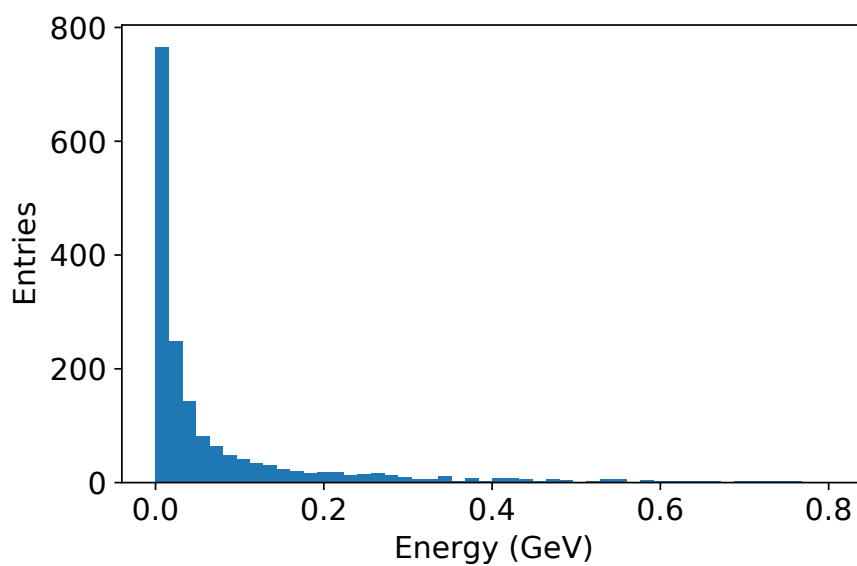


Figure 3.4: Distribution of the bremsstrahlung photon energy in 10,000 Y(4S)-Events.

## 4. New Approach on Bremsstrahlung Finding

In connection with the update of the particle accelerator, the Belle detector to Belle II and the associated rewriting of the software a new method for bremsstrahlung finding is developed. After giving a short overview about the method used at the Belle experiment, a new approach on bremsstrahlung reconstruction is described in this chapter and the current implementation of this idea is described in detail.

### 4.1 The Belle Recovery Method

At Belle the bremsstrahlung photon recovery was done during the offline reconstruction. All ECL clusters, which were not related to a track, located within a cone around the perigee of the trajectory, were collected. The energy deposited in these ECL clusters was then added at the reconstructed origin of the track. The momentum of the electron was then given by

$$p_e = p_e^{\text{tracking}} + \sum p_\gamma$$

Especially for photons radiated far from the interaction point, these approach is expected to have a low finding efficiency. This expectation gets verified later in Section 5.3 and therefore a more efficient method for finding bremsstrahlung photons should be developed.

### 4.2 Idea

The aim for Belle II is to find a more efficient way for bremsstrahlung recovery. In general the idea is to make a two step approach:

- Collect the lost energy by bremsstrahlung with information of the ECL
- Do a refit of the track with the collected information

For each hit measurement of a given track, an extrapolation is done on a straight line in the tracks direction at this track point. The extrapolation is only performed at this hits, because bremsstrahlung only occurs at dense material in the inner detector layers. The position of this dense material also presents the location of the measured hits. The extrapolation then stops at the ECL and it is checked if the endpoint of the extrapolation

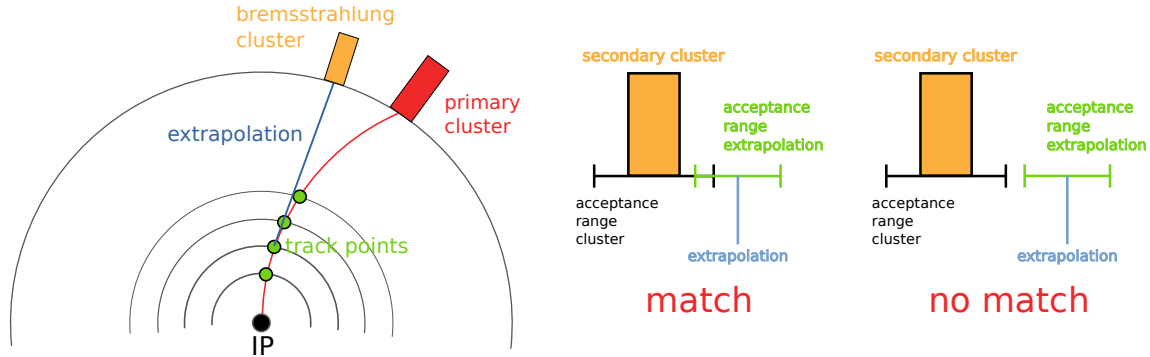


Figure 4.1: Idea for finding bremsstrahlung in the Belle II detector.

matches the position of a secondary ECL cluster (a cluster which is not already associated to a track). The matching is done by assigning an acceptance range to both the cluster and the extrapolation. It is then checked if the acceptance ranges overlap or not. If there is an overlap, the ECL cluster is assumed to be a bremsstrahlung cluster, which was generated by a photon radiated from the original electron. The found cluster then gets associated with the primary ECL cluster, which was produced by the electron. The idea is also shown in Figure 4.1.

The acceptance range which is assigned to the cluster and the extrapolated position depends on two parameters: The error on the position and an acceptance factor, which can be chosen by the user.

One of the expected benefits of this approach is that the lost energy via bremsstrahlung can be added more exactly at the point the radiation happened and not all at the perigee like it was done in the method used at Belle. So a more accurate track fit can be expected.

### 4.3 ECL Position Resolution

For the given approach to be effective a good position resolution of the ECL is needed, so the found energy can be added to the electron energy at the correct layer of the tracking detector. Therefore in this section it is tested which characteristics the electron has to possess, so photons, which were radiated at different layers, can be distinguished in the ECL.

The problem can be simplified by looking for electrons with a trajectory in the x-y-plane. Additionally the layers of the tracking detectors and the ECL wall are approximated as perfect circles. In Figure 4.2 a draft of the simplified problem is given.

The distance between the hits on the ECL of two photons which were radiated at different layers only depends on the curvature of the track. The curvature is given by

$$\omega = \frac{q}{p_t \cdot \alpha}$$

As it can be seen in this formula, the only variable parameter is the transverse momentum of the electron. Because of that, the aim is to get a formula for the distance between the ECL hits, depending on the transverse momentum of the electron.

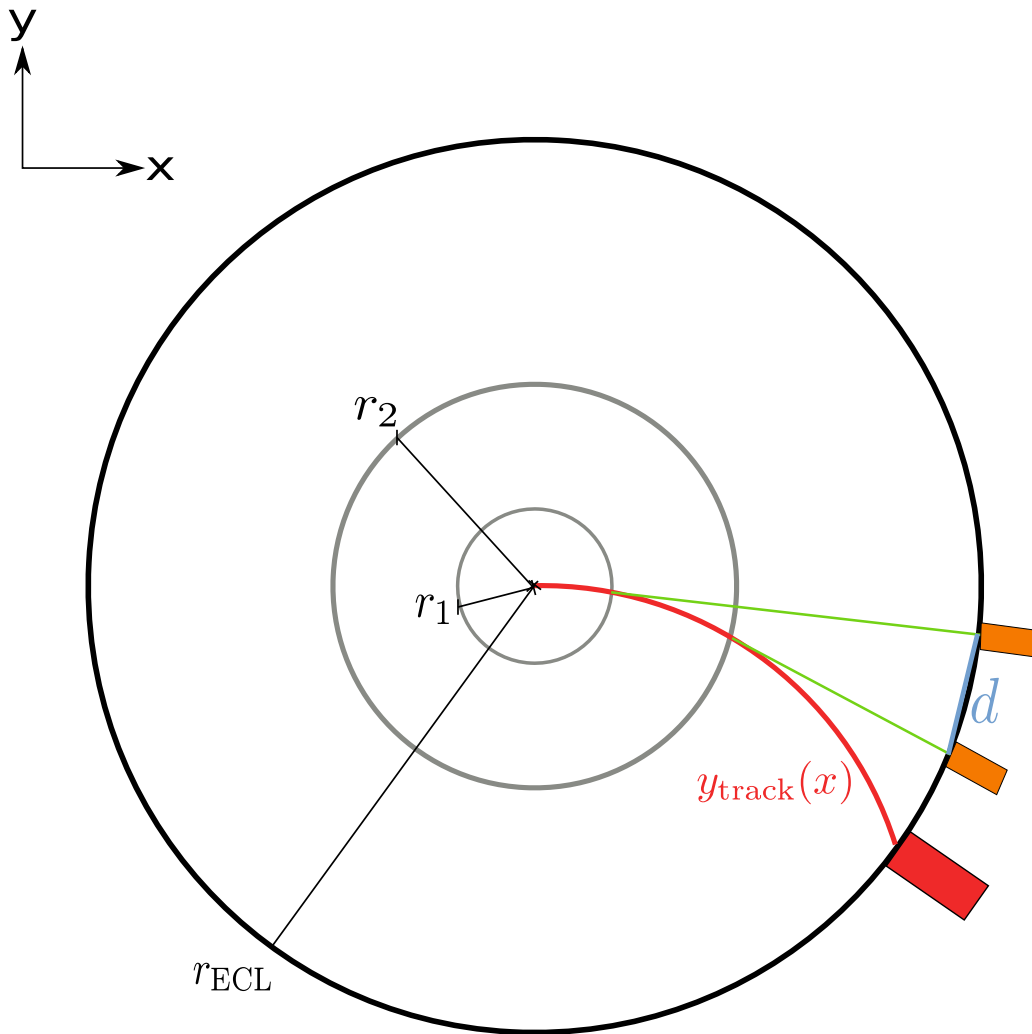


Figure 4.2: Simplified draft for the evaluation of the distance  $d$  between ECL hits, generated by two photons, which were radiated at different VXD layers. The grey circles represent the VXD layers. The ECL wall is presented as black circle. The electron track is shown in red and the tracks of the two radiated bremsstrahlung photons are represented by the green lines. The boxes represent the primary ECL cluster (red) and the bremsstrahlung clusters (orange).

Another assumption that is made in this calculation is, that the slope of the electron track at the origin is  $m = 0$ . This assumption simplifies the calculation and can be made because of the cylinder symmetry of the problem.

The equation of motion for a electron in the detector is given by

$$y_{\text{track}}(x) = \sqrt{R^2 - x^2} - R$$

where  $R = \frac{1}{\omega}$  is the radius of the electron track. Defining  $r_1, r_2$  as the radii of the tracking detector layers, the position on the detector layers is defined by

$$\begin{aligned} y_{\text{layer1}}(x) &= \sqrt{r_1^2 - x^2} \\ y_{\text{layer2}}(x) &= \sqrt{r_2^2 - x^2} \end{aligned}$$

With this information the intersection points of the electron track and the layers can be determined:

$$\begin{aligned} x_{\text{intersection1}} &= \frac{\sqrt{4R^2 - r_1^2 r_1}}{2R} \\ y_{\text{intersection1}} &= \frac{1}{2} \sqrt{4R^2 - \frac{(4R^2 - r_1^2) r_1^2}{R^2}} - R \\ x_{\text{intersection2}} &= \frac{\sqrt{4R^2 - r_2^2 r_2}}{2R} \\ y_{\text{intersection2}} &= \frac{1}{2} \sqrt{4R^2 - \frac{(4R^2 - r_2^2) r_2^2}{R^2}} - R \end{aligned}$$

From this points the bremsstrahlung photons are radiated tangential to the electron track and are moving in straight lines to the ECL. So to give a equation for the movement of the photons, the gradient of the electron track at the layers is needed. With the photon equation of motion it is possible to determine the positions, where the photons hit the ECL. In the last step the distance between these two hits can be determined by the formula

$$d = \sqrt{(x_{ECL2} - x_{ECL1})^2 + (y_{ECL2} - y_{ECL1})^2}$$

To simplify the result a taylor expansion was done, leading to the formula for the distance  $d$  between the hits

$$d \approx C_1(r_1, r_2) \cdot \omega + C_2(r_1, r_2) \cdot \omega^3 + \mathcal{O}(\omega^5)$$

Here  $C_1$  and  $C_2$  are coefficients depending on which layers are tested. A complete list of the coefficients is given in Table 4.1.

To make a statement as to, whether the ECL position resolution is good enough to assign the photon radiation to the correct layer or not, the distance between the hits has to be

Table 4.1: Coefficients for the calculation of the distance between photon hits in the ECL.

Inner Layer	Outer Layer	$C_1$	$C_2$
3	4	449.82	1854.89
3	5	811.20	5156.82
3	6	1061.82	8742.56
4	5	361.37	4592.78
4	6	612.00	9749.17
5	6	250.62	5699.00

compared with the position resolution. The position resolution of the ECL is approximated by

$$\Delta d = \frac{w_{\text{ECL}}}{\sqrt{12}} \text{ cm}$$

in this thesis, with  $w_{\text{ECL}}$  being the width of a ECL crystal which is 6 cm. In the experiment the ECL position resolution is even better, because of some tricks in the reconstruction software. But for this thesis the approximation is exact enough.

In Figure 4.3 the distance between the ECL hits of the radiated bremsstrahlung photons is plotted over the transverse momentum of the electron. The ECL position resolution can be found in this plot, as well. For momenta where the curve is above the ECL resolution line, the photon radiation vertex can be assigned to the correct tracking detector layer. For momenta below the resolution line it can not be guaranteed that the radiation vertex is assigned correctly.

As it can be seen in the plot, for low electron momenta a good assignment to the correct layer is possible, whereas for electrons with a high transverse momentum the reconstruction of the radiation vertex becomes more difficult. The reason for this is the low curvature of these tracks, which results in a short distance between the potential photon hits in the ECL. If this distance becomes too short, it is not possible to differentiate them in the ECL, due to the limited position resolution.

After getting information about the momentum range, where a good assignment is possible, the momentum distribution of the electrons in the experiment has to be analyzed, to get knowledge about the number of cases where the approach could work properly. Therefore the distribution of the transverse momentum of electrons in Y(4S) events was plotted in Figure 4.3, as well. As it can be seen in the plot, the largest amount of electrons are in the momentum range where the position resolution of the ECL should be good enough for the approach to work.

## 4.4 Implementation

Due to the fact that the position resolution of the ECL seems to be good enough to realize the given idea of bremsstrahlung finding, the approach is implemented in the module called

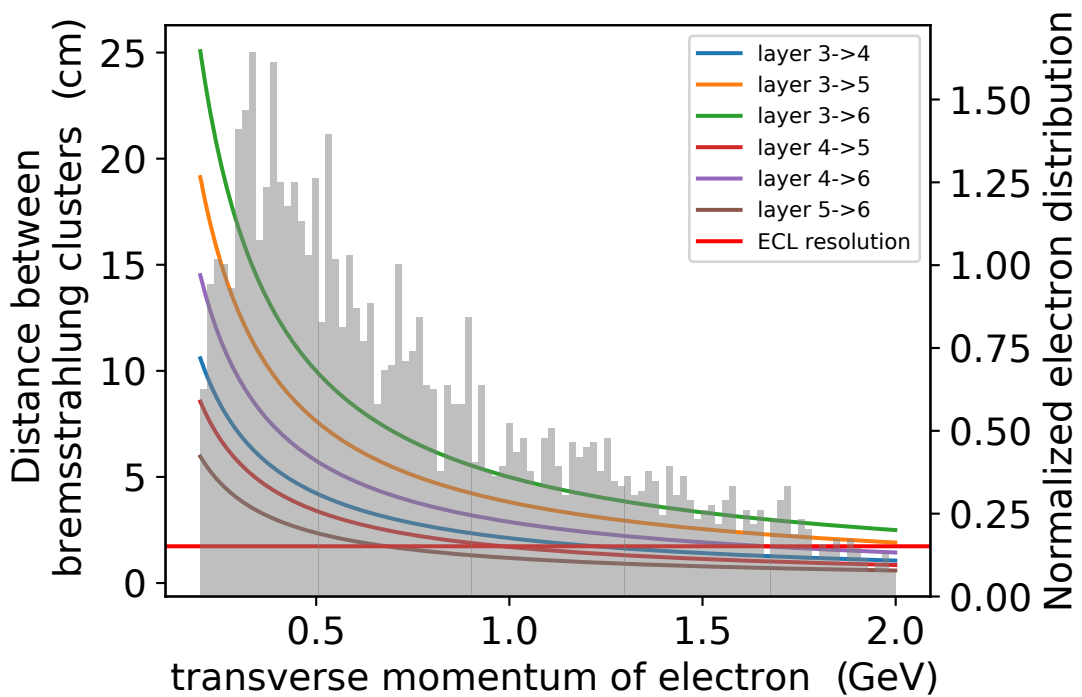


Figure 4.3: Distance between photons, radiated at different layers, hitting the ECL. The ECL position resolution is plotted in red for comparison. Electron transverse momentum distribution taken from 10,000 Y(4S) events.

**ECLTrackBremFinder** in the basf2 code. In this section the developed algorithm is described in detail.

For a better understanding of the current implementation, the concept of a relation, set by modules of the software framework, is explained in this paragraph. Relations are used to link different elements from the Data Store with each other. As an example, the software can match tracks and ECL clusters, if the cluster is expected to be generated by the same particle as the hits in the tracking detectors. Relations are also saved in the Data Store and can be set and called up by every module of the framework. So in the current implementation of the bremsstrahlung finding algorithm, relations are used to make the link between the bremsstrahlung cluster and the primary ECL cluster, generated by the original particle.

For each single event, the module loops over all tracks saved in the Data Store. For each of these tracks the related RecoTrack is taken from the Data Store. In the ideal case, there should be a ECL cluster related to the track. This cluster was assumed to be generated by the same particle as the track and is therefore set as the primary cluster in the algorithm. When searching for the primary cluster the algorithm has to check the Cluster Hypothesis ID, because every cluster is saved with two different hypotheses, one for electrons and one for photons. The module then takes the cluster with the electron hypothesis. In the case where either no RecoTrack or primary cluster is found, the module continues with the next track.

After the primary cluster was found, a loop over all ECL clusters is performed, to find candidates of clusters which could have been generated by bremsstrahlung photons. These candidates are called secondary clusters from now on. As secondary cluster only the ones, which are compatible with a photon particle hypothesis and are not already associated to a different track, are selected. If a cluster, which meets both requirements, is found, the cluster gets checked if the position suits the trajectory of the track.

Like described in Section 4.2, this check is done by extrapolating each track point in a straight line to the edge of the ECL. As direction for the extrapolation the gradient of the track at this point is used, because the bremsstrahlung photons are emitted tangential to the electrons direction. Therefore the  $\phi$  and  $\theta$  angle of the fitted momentum of each VXD track point gets compared with the angles of the cluster.

To get a higher efficiency and better accuracy when assigning the radiation vertices, three virtual hits are generated in addition to the original VXD hits. One of this virtual hits represents the edge of the beam pipe where, as it can be seen in Figure 4.4, a large amount of bremsstrahlung photons are radiated. The other two virtual hits are generated at  $\rho = 15\text{ cm}$  and  $\rho = 16\text{ cm}$  and constitute the inner CDC wall. The virtual hits are handled like the normal VXD hits. That means they are extrapolated to the ECL and the position of the extrapolation is compared with the cluster position.

If a match is found, the secondary cluster and the track point are paired and stored in a result list. From all pairs in this list, the one with the smallest angular deviation between the extrapolation and the cluster position is chosen.

Finally, the module sets a relation, like described at the beginning, between the suspected bremsstrahlung photon cluster and the primary cluster of the track. Every track point has a sorting parameter, which can here be seen as a enumeration of the track point. This sorting parameter is saved together with the relation. With this information the position of the photon radiation can be reconstructed in the analysis by simply taking the position

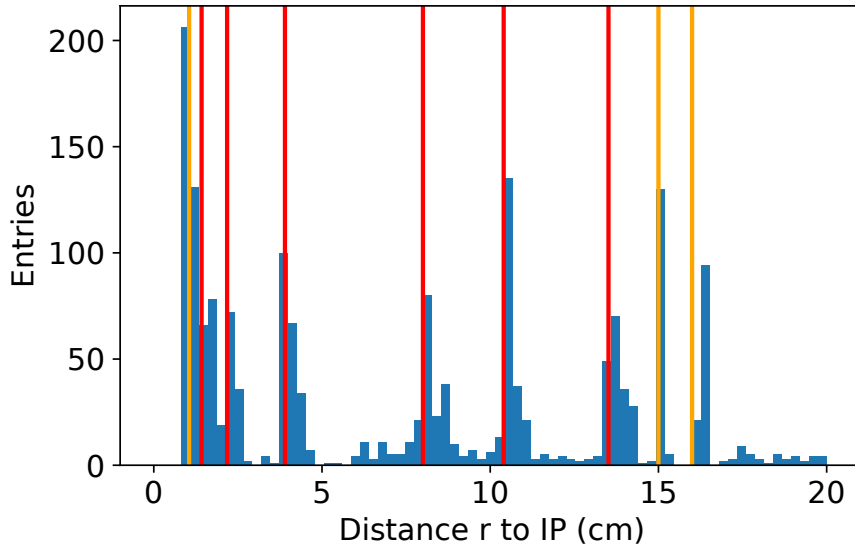


Figure 4.4: Distribution of the bremsstrahlung photons vertices over the radial distance to the detector center  $\rho$ . The radii of the VXD layers are presented in red, the ones of the virtual hits in orange.

of the track point with the given sorting parameter from the Data Store. Then the lost energy can be added at this position, what should lead to an improved track fit and an improved energy reconstruction.

## 5. Evaluation

The next step, after describing the algorithm, is testing how good the ability of the module in finding bremsstrahlung photons is. Therefore the module gets tested how its functionality behaves under several parameters, like for example the dependency on the energy of the original electron or the bremsstrahlung photon.

### 5.1 Module Efficiency

To verify the functionality of the module, two numbers are taken into account. For a module with the purpose of finding bremsstrahlung photons, the most interesting number is the percentage of photons, which are found. Also the number of clusters, which were falsely related to another cluster, the so called fake rate, is of interest.

The efficiency of the module is defined with the following formula

$$\text{Efficiency} = \frac{\# \text{ secondary cluster with correct relation}}{\# \text{ bremsstrahlung photons with cluster}}$$

This formula arises from the fact that in the experiment, photons can only be detected over the ECL clusters generated by them. Because of this the number of clusters, which got related to the correct primary ECL cluster by the algorithm, is standing for the number of correctly found bremsstrahlung photons. When calculating the efficiency only the bremsstrahlung photons, with a energy high enough to generate a hit in the ECL, are considered. The reason for this is the fact that the algorithm cannot find photons, which do not generate a cluster. But this problem could only be solved with a lower energy threshold in the ECL and should therefore not been taken into account when evaluating the functionality of the module.

The first variable the efficiency is depending on, is the choice of the acceptance factor. In Table 5.1 the dependency of the efficiency on the acceptance factor is shown. As it is clearly visible, the efficiency is rising for a larger acceptance factor. The reason for this is the fact that a higher acceptance factor is resulting in a bigger acceptance range and therefore an overlap between the acceptance range of the cluster and the extrapolation becomes more probable.

By increasing the acceptance factor, the number of found bremsstrahlung photons and therefore the efficiency is getting better. But the other interesting number for the evaluation, the fake rate, also is increasing with a higher acceptance factor, as it can be seen in Table 5.1. For the fake rate, which specifies the percentage of ECL clusters, which

Table 5.1: Efficiency and Fake Rate of the bremsstrahlung finding module depending on the Acceptance Factor. Results are based on 10,000 Y(4S)-Events without considering background.

Acceptance Factor	Efficiency [%]	Fake Rate [%]
1.0	50.32 $\pm 1.78$	8.70 $\pm 0.90$
2.0	78.00 $\pm 2.08$	13.76 $\pm 0.85$
3.0	86.47 $\pm 1.94$	17.87 $\pm 0.90$
4.0	89.00 $\pm 1.85$	21.21 $\pm 0.97$
5.0	89.63 $\pm 1.82$	24.37 $\pm 1.03$
6.0	90.52 $\pm 1.77$	26.97 $\pm 1.07$

are falsely marked as bremsstrahlung clusters, a low value is desirable. The fake rate is specified by

$$\text{Fake Rate} = \frac{\# \text{ secondary cluster with wrong relation}}{\# \text{ cluster with relation}}$$

Logically the number of wrongly collected clusters is becoming higher, when making the acceptance range bigger. Because of that, the target is to find a acceptance factor, which strikes a balance between the efficiency becoming as high as possible and minimizing the fake rate.

By taking a look on the data in Table 5.1, an acceptance factor of 3.0 becomes sufficient. From this factor on the fake rate is increasing more than the efficiency, what can also be seen in Figure 5.1. Therefore this acceptance factor was chosen for the following validation of the module.

### 5.1.1 Efficiency and Fake Rate depending on Electron Energy

For the validation of the module, it is of interest, if the photon finding efficiency is depending on the energy of the primary electron. Therefor in Figure 5.2 the relation between efficiency and electron energy is plotted. As it can be seen, the efficiency is slightly increasing with a higher energy of the electrons. This can be explained by the fact that the track fit becomes more precise for high energetic particles. Since the bremsstrahlung finding module uses the fitted track points as starting point for the extrapolation to the ECL, a higher accuracy in the track fit also results in a higher accuracy in the extrapolation and therefore the chance that the acceptance range of cluster position and extrapolation overlap gets higher.

Figure 5.2 also shows the Fake Rate falling for higher electron energies. Cause for this is the lower curvature of high energetic tracks. Due to the fact that the algorithm is extrapolating from each track point, a larger phase space gets checked if the curvature of the track is larger. This fact is also explained in Figure 5.3. The probability for collecting a secondary cluster, which does not belong to a bremsstrahlung photon radiated by the

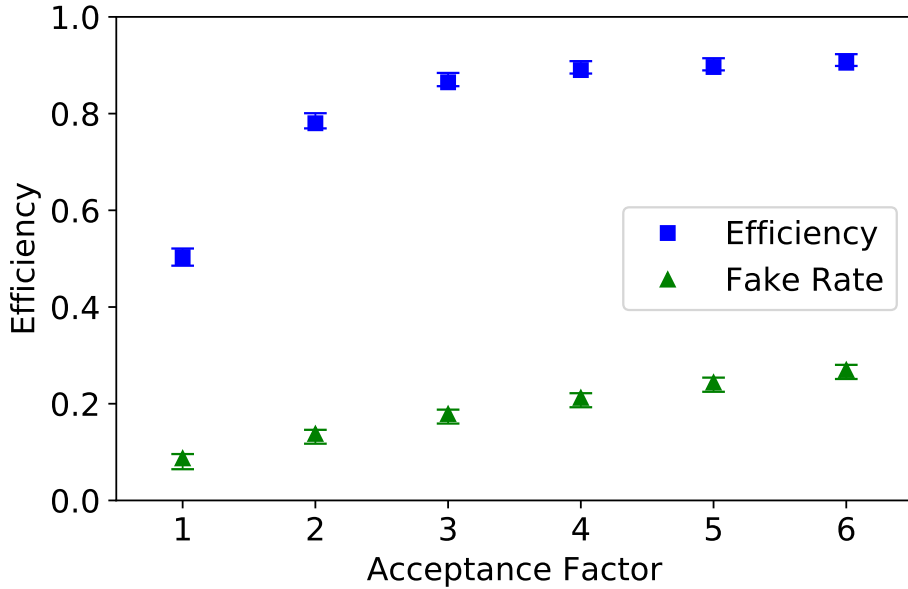


Figure 5.1: Efficiency and Fake Rate of the module depending on the Acceptance Factor, based on 10,000 Y(4S)-Events

primary electron, is higher when searching in a larger area.

Combining the tendency of the Efficiency and the Fake Rate, the conclusion can be made, that the module works better for high energetic electrons and positrons.

### 5.1.2 Efficiency depending on Photon Characteristics

Another interesting relation, which has to be checked, is the one between the bremsstrahlung photon finding efficiency and the characteristics of the photons, like photon energy and radiation vertex.

So first the capability of the module for finding the photons, when varying their energy is investigated. The ability of the module to find bremsstrahlung photons in the ECL only depends on the position resolution of the ECL and the effectiveness of the track fitting algorithm. Considering that the trajectory of a photon is not affected by its energy and therefore the position of the ECL hit is independent from the photons energy, it can be expected that the efficiency of the module should not be depending on the bremsstrahlung photons energy. This theory gets confirmed by taking a look on the correlation of efficiency and photon energy in Figure 5.4. Nevertheless it has to be respected, that there are only few bremsstrahlung photons, which have an energy bigger than 0.4 GeV. This leads to a high uncertainty in the efficiency calculation in this energy range.

Nevertheless, if an electron is emitting more than one bremsstrahlung photon, the energy of the first emitted photon is affecting the probability of finding the others. The reason for this is in the correlation of efficiency and electron energy. Radiating a photon results in a kink in the electron trajectory because of the energy loss. This means, by taking a look on Section 5.1.1, the more energy the electron is losing, the more unlikely other photons

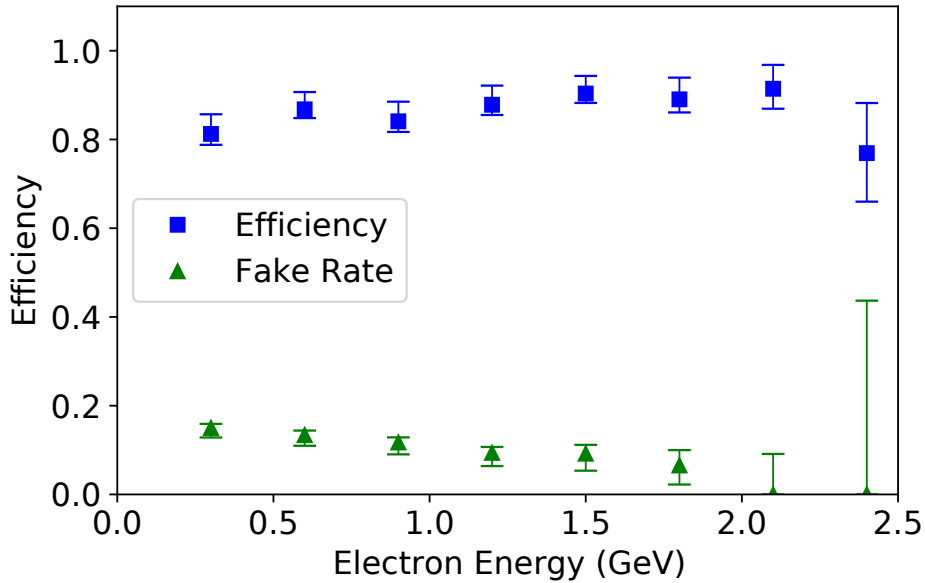


Figure 5.2: Efficiency and Fake Rate of the bremsstrahlung finding module depending on the energy of the primary electron. The results are based on 10,000 Y(4S)-Events and were created with an acceptance factor of 3.0.

emitted by the same electron will be found.

One of the aims when developing the module was to achieve a finding efficiency which is independent of the radiation vertices of the bremsstrahlung photons. When taking a look on Figure 5.5 it can clearly be seen that this goal was achieved with the current implementation of the module.

## 5.2 Photon Vertex Reconstruction

One of the main improvements of the bremsstrahlung finding algorithm in comparison to the Belle method is the ability to add the lost energy at the point the radiation happened. It is therefore from large interest if the module assigns the radiation vertex to the correct VXD layer and therefore to the correct position. The module saves the sorting parameter of the track point where the extrapolation and the cluster position have the best accordance. With this information it is possible to reconstruct the radiation vertex of the photon in the analysis. By comparing this reconstructed vertex with the Monte Carlo information from the simulation, the accuracy of the assignment can be checked. In Figure 5.6 the distance between the reconstructed photon vertices and the original photon radiation vertices based on Monte Carlo information is plotted. As it can be seen in this plot, the assigned hit only slightly differs from the simulated radiation vertex in most cases. To be more specific, a percentage of about 68% of all found bremsstrahlung photons get assigned within a range of 5 cm around the Monte Carlo Vertex. In some cases it occurs that the assigned position and the true position based on Monte Carlo information differ from each other by more

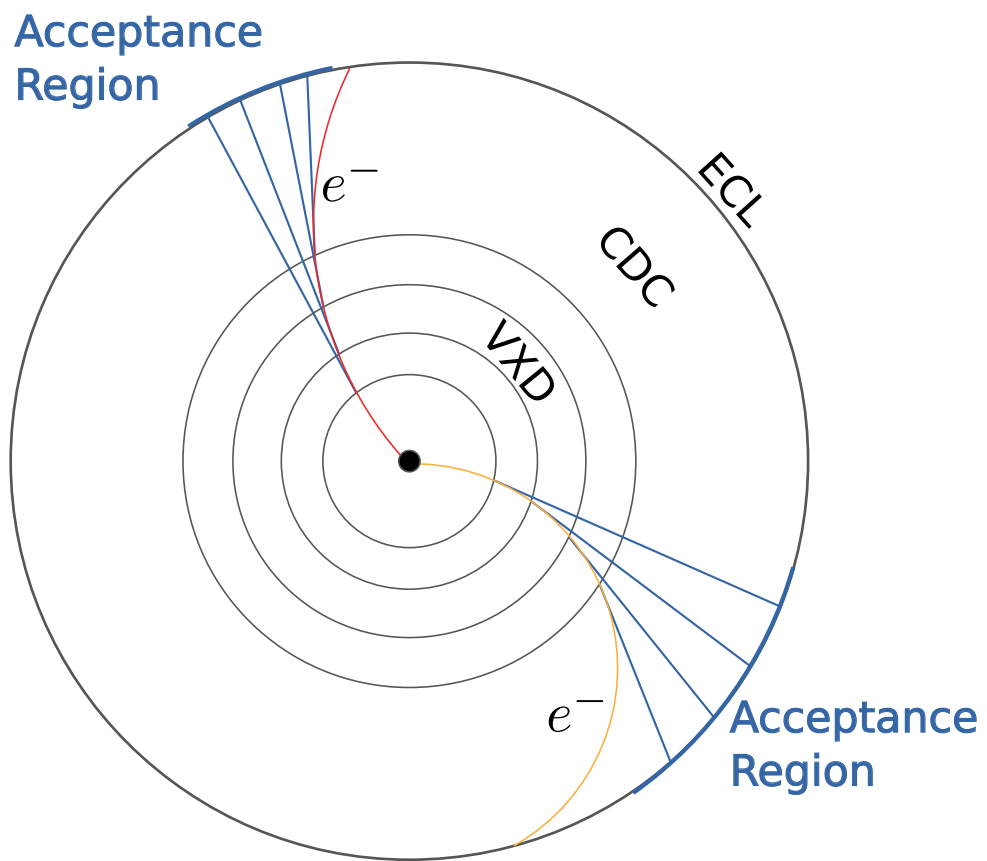


Figure 5.3: Acceptance region of the bremsstrahlung finding module depending on the curvature of the track.

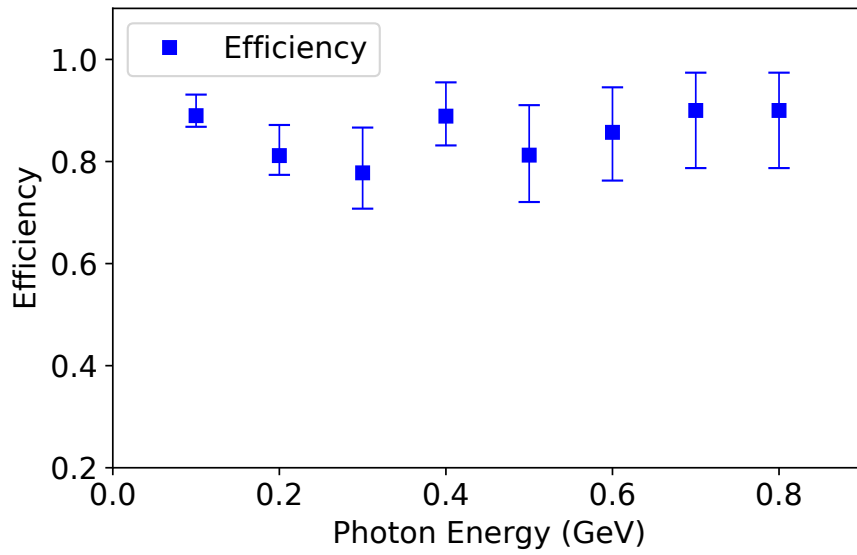


Figure 5.4: Correlation of the bremsstrahlung finding efficiency and the photon energy, based on 10,000 Y(4S)-Events with an acceptance factor of 3.0.

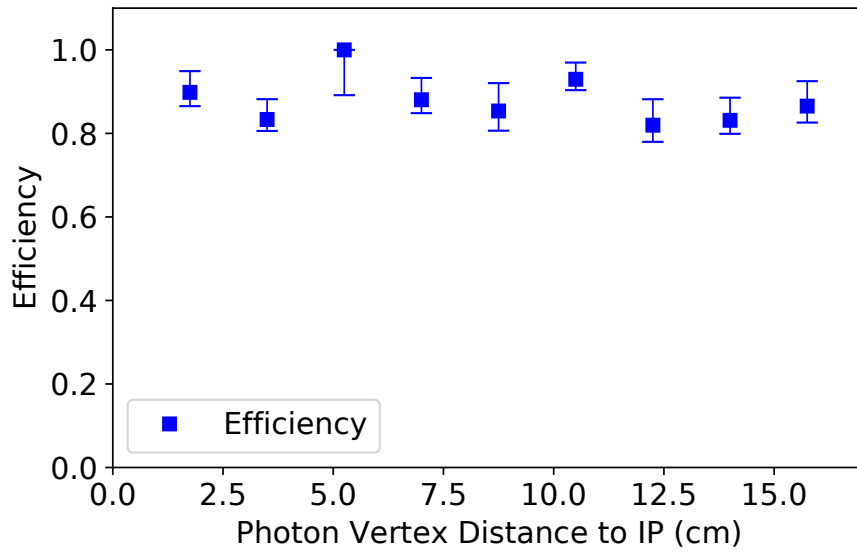


Figure 5.5: Correlation of the bremsstrahlung finding efficiency and the photon vertex, based on 10,000 Y(4S)-Events with an acceptance factor of 3.0.

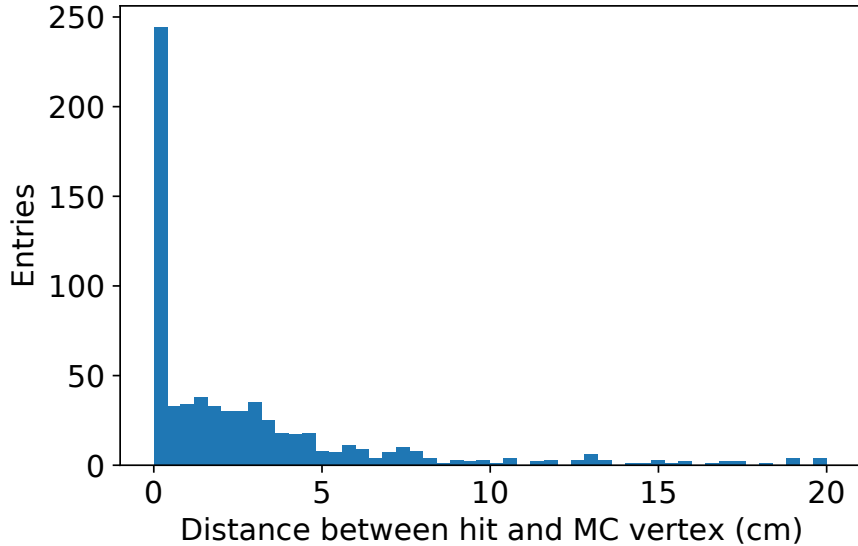


Figure 5.6: Distance between the hit that gets assigned by the bremsstrahlung finding module and the original radiation vertex, which is based on Monte Carlo information.

than 10 cm. This can be explained by high energetic electron tracks, which have such a slight curvature, that a correct assignment becomes unlikely, like described in Section 4.3.

### 5.3 Comparison to the Belle Method

With the information about the efficiency correlating with several characteristics of the primary electron and the bremsstrahlung photons, it is possible to compare the performance of the method with the one used for some analyses at the Belle experiment, described in Section 4.2.

One of the main goals, when developing the new algorithm, was achieving a higher finding efficiency compared to the old Belle method. As it can be seen in Figure 5.7 this requirement is fulfilled. It is noticeable that especially at low electron energies, the new method is performing way better. This can be explained by the high curvature of low momentum tracks, which leads to the problem that primarily bremsstrahlung photons, which are radiated far from the interaction point, can not be detected, because they are not lying in the cone which starts at the perigee. The probability that the ECL hits of the bremsstrahlung photons lie in this cone is increasing for higher electron energies, because of the lower curvature in this cases. This problem is solved by extrapolating from every single track point and not only from the perigee of the track, in the new approach. This leads to a finding efficiency which is nearly independent from the primary electrons energy, compared to the one of Belle.

Comparing the fake rate of both methods, it can be seen that the new approach has a significantly lower fake rate than the one from Belle.

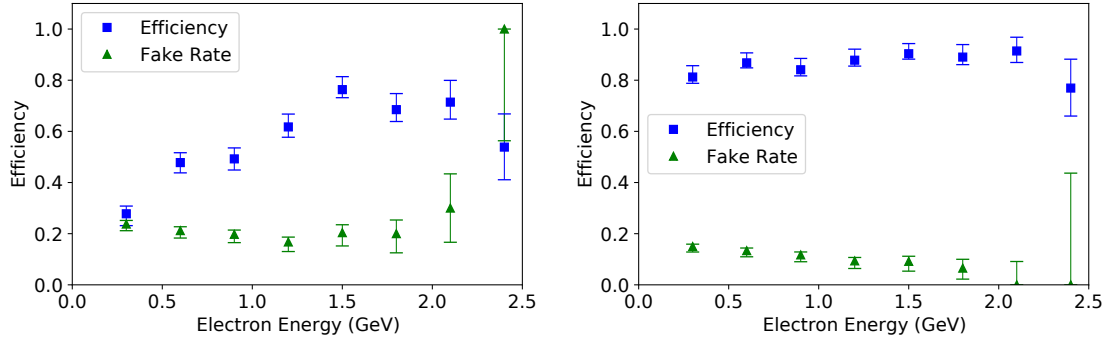


Figure 5.7: Comparison of the bremsstrahlung finding efficiency and fake rate, depending on the energy of the primary electron, between the new approach for Belle II and the Belle method. Left side: Belle method with a cone angle of  $5^\circ$ . Right side: Belle II approach with an acceptance factor of 3.0.

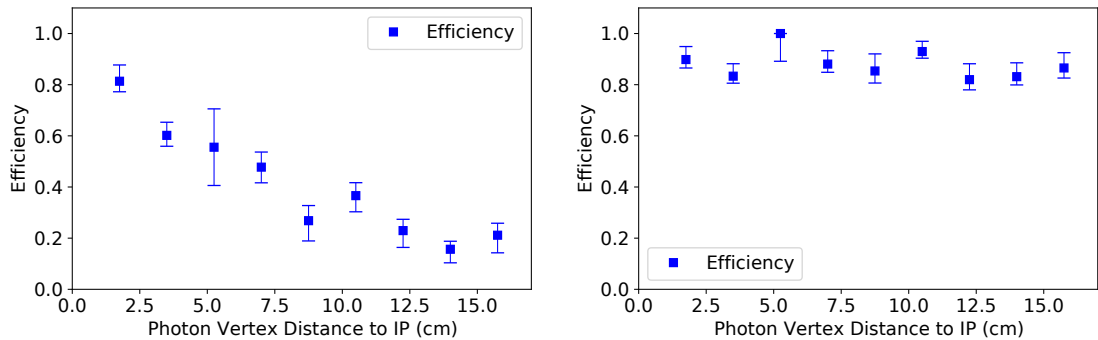


Figure 5.8: Comparison of the bremsstrahlung finding efficiency, depending on the bremsstrahlung photon vertices, between the new approach for Belle II and the Belle method. Left side: Belle method with a cone angle of  $5^\circ$ . Right side: Belle II approach with an acceptance factor of 3.0.

One of the problems with the Belle method was, that in particular for low energetic tracks it was not possible to find bremsstrahlung photons, which were radiated at outer layers in the VXD. This problem is shown in Figure 5.8. Drawn from the comparison between the old and the new method the conclusion can be made that this problem is solved with the implementation, developed in this thesis.

## 6. Summary

To make relevant conclusions with the data taken by the Belle II detector a good energy resolution is desirable. Thereby the bremsstrahlung recovery plays an important role when trying to improve the energy resolution, because bremsstrahlung is the dominant effect for the energy loss of electrons at the energies occurring in the detector.

This thesis introduces a new approach on bremsstrahlung finding, using the information from the ECL and reconstructed tracks. The new method represents a considerable improvement over the one mostly used during offline reconstruction at the Belle experiment. The bremsstrahlung photons, radiated by electrons and positrons in the detector, are mostly emitted at the single layers of the vertex detector (VXD). Also, bremsstrahlung radiation takes places at the edge of the beam pipe and at the inner wall of the Central Drift Chamber.

At this point the new approach comes in. The fact that electron creates a track point at each of these layers, leads to the idea of extrapolating from each of this track points to the ECL, checking if the extrapolation matches the position of an ECL cluster. This cluster then gets assigned as a bremsstrahlung cluster, created by an emitted photon, and the lost energy can be added at the track points position. However the current implementation of the idea only makes a link between the cluster created by the electron and the found bremsstrahlung cluster, not adding the missing energy to the electron. Consequently one of the main tasks to follow should be the implementation of the bremsstrahlung finding module in the track fitting algorithm.

Evaluating the new developed module shows that the ability of finding bremsstrahlung photons is much better than with the method used at Belle. With the new approach it is possible to find about 86 % of all bremsstrahlung photons, which create a cluster in the ECL. This is an improvement of about 30 % more found photons than before. Especially the dependency of the finding efficiency on the radiation vertex of the bremsstrahlung photons is eradicated with the developed method. In particular that makes the finding efficiency of photons emitted by low momentum electrons way better than at Belle.

When rating the finding efficiency it should be taken into account, that there is one problem when calculating the efficiency. If different bremsstrahlung photons are matched to the same ECL cluster, because the hits are close together, only one of them is counted as a found photon. In this case the energy of two photons is assigned at one point and not like it should be at two different track points. Also this leads to the fact that the finding efficiency is expected to be a little bit higher than calculated in this thesis. This problem could be solved with a better spatial resolution of the ECL, what also would lead to a better match-

ing of bremsstrahlung cluster and photon radiation vertex. Nevertheless the assignment of the missing energy to the actual radiation vertex is possible with this algorithm for the first time and the success rate is good. About 68 % of all found bremsstrahlung photons where assigned within a range of 5 cm around the vertex known from the simulated Monte Carlo information.

Another improvement which could be done to the algorithm is the way the clusters are assigned to the position of the radiation. The current implementation of giving the sorting parameter of the track point as weight to the relation between the ECL cluster, generated by the electron, and the bremsstrahlung cluster is only a workaround to the problem. A better solution would be the setting of a relation between the bremsstrahlung cluster and the track point itself.

The algorithm also generates a smaller number of falsely as bremsstrahlung cluster marked clusters. With a fake rate of about 18 % it performs better than the previous method.

Summarized the developed method performs better on every tested criteria. Therefore it is expected to get an improved energy resolution in the Belle II experiment, after including the module in the track fitting algorithm. Then the influence of the algorithm on the vertex reconstruction of the primary particles can be investigated. It is expected that the vertex reconstruction will get better, due to the recovery of the bremsstrahlung energy, but this fact has still to be tested.

# Bibliography

- [1] **Belle**, K. Abe *et al.*, “Observation of large CP violation in the neutral  $B$  meson system,” *Phys. Rev. Lett.* **87** (2001) 091802, [arXiv:hep-ex/0107061 \[hep-ex\]](https://arxiv.org/abs/hep-ex/0107061).
- [2] **Belle-II**, T. Abe *et al.*, “Belle II Technical Design Report,” tech. rep., KEK, 2010. [arXiv:1011.0352 \[physics.ins-det\]](https://arxiv.org/abs/1011.0352). [http://arxiv.org/pdf/1011.0352v1](http://arxiv.org/pdf/1011.0352v1.pdf).
- [3] Belle II, “SuperKEKB and Belle II.” [https://www.belle2.org/project/super\\_kekb\\_and\\_belle\\_ii/](https://www.belle2.org/project/super_kekb_and_belle_ii/). [online, accessed 24. January 2018].
- [4] DESY, “Belle & Belle II.” <https://belle2.desy.de>. [online, accessed 24. January 2018].
- [5] C. Pulvermacher, “dE/dx Particle Identification and Pixel Detector Data Reduction for the Belle II Experiment,” 2012.
- [6] Jochen Schieck for the DEPFET Collaboration, “DEPFET Pixels as a Vertex Detector for the Belle II Experiment,” *ArXiv e-prints* (Apr., 2013) , [arXiv:1304.0870 \[physics.ins-det\]](https://arxiv.org/abs/1304.0870).
- [7] H. Kolanoski, “Teilchendetektoren : Grundlagen und Anwendungen,” 2016. <http://swbplus.bsz-bw.de/bsz468154302cov.htmhttp://dx.doi.org/10.1007/978-3-662-45350-6>.
- [8] A. Moll, “The software framework of the Belle II experiment,” *J. Phys. Conf. Ser.* **331** (2011) 032024.
- [9] R. Brun and F. Rademakers, “ROOT — an object oriented data analysis framework,” *Nuclear Instruments and Methods in Physics Research Section A: Accelerators, Spectrometers, Detectors and Associated Equipment* **389** no. 1-2, (Apr, 1997) 81–86. [https://doi.org/10.1016/s0168-9002\(97\)00048-x](https://doi.org/10.1016/s0168-9002(97)00048-x).
- [10] E. Haug and W. Nakel, *The Elementary Process of Bremsstrahlung*. World Scientific lecture notes in physics. World Scientific, 2004. <https://books.google.de/books?id=f1H8ngEACAAJ>.
- [11] G. H. Zschornack, *Handbook of X-Ray Data*. Springer Berlin Heidelberg, 2007. <https://doi.org/10.1007/978-3-540-28619-6>.
- [12] S. Eidelmann *et al.*, “Review of Particle Physics,” *Physics Letters B* **592** (2004) 1+. <http://pdg.lbl.gov>.

- [13] M. Prim, “Study of Material Effects in Track Fitting and Improvement of the  $K_S^0$  Reconstruction at Belle II,” 2015.

# Danksagung

Zuletzt möchte ich mich bei allen bedanken, die zum Gelingen dieser Arbeit beigetragen haben.

Zunächst gilt mein Dank Herrn Prof. Dr. Florian Bernlochner, für die Übernahme des Referats.

Für die Übernahme des Korreferats, sowie die intensive Betreuung über den gesamten Arbeitszeitraum und das Korrekturlesen der Arbeit, möchte ich mich bei Herrn Dr. Thomas Hauth herzlich bedanken.

Mein Dank gilt auch Herrn Dr. Martin Heck, für die Betreuung und die umfassenden physikalischen Erläuterungen.

Zudem möchte ich mich bei der gesamten Arbeitsgruppe für das gute und hilfsbereite Arbeitsklima bedanken. Ein besonderer Dank gilt hierbei Nils Braun, Moritz Gelb und Markus Prim, welche mir stets mit Rat und Tat zur Seite standen.

Abschließend möchte ich mich noch bei meiner Familie, vor allem bei meinen Eltern, für die Unterstützung während des gesamten Bachelorstudiums, ohne die dieses nicht möglich gewesen wäre, bedanken.